12798–12807 *Nucleic Acids Research, 2017, Vol. 45, No. 22* *Published online 13 October 2017*
doi: 10.1093/nar/gkx929

CsrA maximizes expression of the AcrAB multidrug resistance transporter

Vito Ricci[1], Victoria Attah[1], Tim Overton[2], David C. Grainger[3] and Laura J.V. Piddock[1,*]

[1]Antimicrobials Research Group, School of Immunity and Infection, College of Medical and Dental Sciences, Institute of Microbiology and Infection, University of Birmingham, Birmingham B15 2TT, UK, [2]Bioengineering, School of Chemical Engineering, University of Birmingham, Birmingham B15 2TT, UK and [3]Institute of Microbiology and Infection, School of Biosciences, University of Birmingham, Edgbaston, Birmingham B15 2TT, UK

Received April 28, 2017; Revised September 26, 2017; Editorial Decision September 28, 2017; Accepted October 02, 2017

ABSTRACT

Carbon Storage Regulator A (CsrA) is an RNA binding protein that acts as a global regulator of diverse genes. Using a combination of genetics and biochemistry we show that CsrA binds directly to the 5′ end of the transcript encoding AcrAB. Deletion of *csrA* or mutagenesis of the CsrA binding sites reduced production of both AcrA and AcrB. Nucleotide substitutions at the 5′ UTR of *acrA* mRNA that could potentially weaken the inhibitory RNA secondary structure, allow for more efficient translation of the AcrAB proteins. Given the role of AcrAB-TolC in multi-drug efflux we suggest that CsrA is a potential drug target.

INTRODUCTION

Efflux pumps that belong to the resistance-nodulation division (RND) family, found in Gram-negative bacteria, confer intrinsic and acquired multi-drug resistance (MDR) in clinically relevant infections (1). Of the RND efflux pumps, the tripartite AcrAB–TolC complex is best characterized. Regulation of AcrAB expression is best understood at the level of transcription initiation in *Escherichia coli* and *Salmonella enterica* serovar Typhimurium. Hence, the local regulator AcrR, and global regulator RamA, repress and activate *acrAB* transcription respectively (2). Other AraC-type transcription factors, closely related to RamA, can influence levels of AcrAB–TolC (3). Hence, MarA, SoxS and Rob recognize the same DNA target as RamA and have overlapping regulatory effects (Figure 1). It has also been shown that expression of *ramA* is increased by mutational inactivation of *acrAB* or when efflux is inhibited (4). It is unknown if AcrAB–TolC expression is also controlled post-transcriptionally.

Carbon storage regulator A (CsrA) is an extensively studied RNA binding protein homologous to the *Pseudomonas fluorescens* repressor of secondary metabolites A (RsmA) protein (5). Initially identified in *E. coli* K-12, CsrA is a 61-amino acid, dimeric RNA-binding protein that targets sites in RNA molecules (15,17–19). Studies have shown that the primary consensus motif A(N)GGA is required for high affinity binding of CsrA to target mRNA (6–9). CsrA sites that deviate from the consensus are termed secondary and bind CsrA with lower affinity (10). Hence, CsrA can modulate translation and transcript stability by controlling access to the ribosome or RNA cleavage factors such as RNase E (11–14).

In our study, we set out to identify factors involved in regulation of *ramA*. To do this we used a *ramA* promoter-GFP reporter plasmid and a transposon library of *S*. Typhimurium SL1344. Using fluorescence-activated cell sorting (FACS), bacteria with increased fluorescence were isolated and genome sequencing identified genes conferring increased *ramA* expression. Surprisingly, inactivation of *csrA*, not previously implicated in control of *ramA,* increased *ramA* expression. We determined that induction of *ramA* in the *csrA* mutant was indirect and required CsrA binding to the *acrAB* transcript. This enhances AcrAB expression and so stabilizes the *acrAB* mRNA. To our knowledge, this study provides the first evidence for regulation of multi-drug efflux and resistance by CsrA.

MATERIALS AND METHODS

Bacterial strains and plasmids

The strains and plasmids used in this study are shown in Supplementary Table S1. *Salmonella enterica* serovar Typhimurium strain SL1344 was used throughout unless indicated otherwise. Mutants of SL1344, lacking functional *acrA*, *acrB*, *ramA, ramR* or *csrA* genes, were constructed using the method of Datsenko and Wanner (15). Complementation of the *csrA* mutant was done using a low copy number vector pWSK30. The GFP transcriptional fusions were made using the method described by Lawler *et al.* (4). Hence, DNA fragments carrying the *ramA* or*acrAB* promoter region, flanked by BamHI and XbaI restriction sites, were cloned into the GFP reporter pMW82. Bacteria

*To whom correspondence should be addressed. Tel: +44 121 414 6966; Fax: +44 121 414 6814; Email: l.j.v.piddock@bham.ac.uk

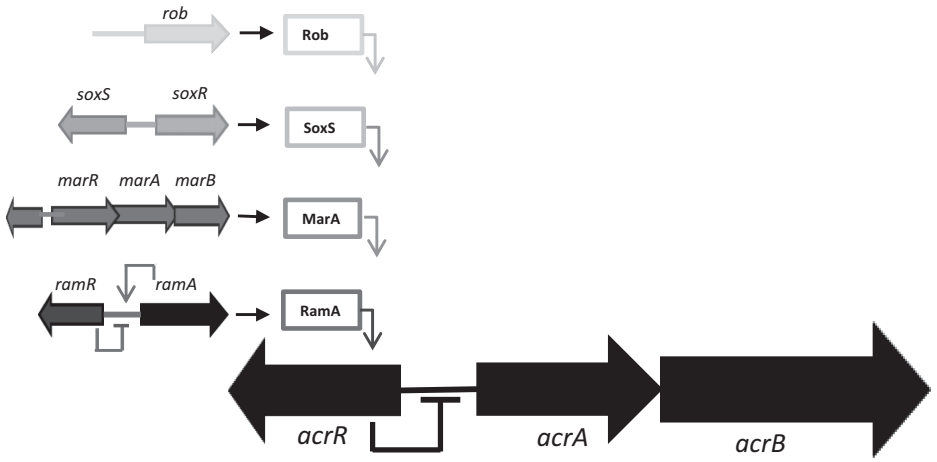

Figure 1. Transcriptional regulation of *acrAB* expression in *Escherichia coli* and *Salmonella enterica*. In both *E. coli* and *S. enterica* the *acrAB* regulon (•) can be activated by the transcriptional activators, MarA (•), SoxS (•) and Rob (•). In S. *enterica ramRA* (•) is the master regulator of the *acrAB* regulon. MarA, SoxS, Rob and RamA activate the *acrAB* regulon by directly binding to a degenerate nucleotide sequence upstream of the *acrAB* locus known as the mar/sox/rambox. In *E. coli* and *S. enterica acrR* is the local repressor of *acrAB*, in *S. enterica ramR* acts as the local repressor of *ramA*.

were routinely cultured in Luria–Bertani broth (LB). Sigma Aldrich supplied all chemicals and antibiotics, unless otherwise stated.

Fluorescence-activated cell sorting (FACS) methodology

The *S.* Typhimurium SL1344 TraDIS library, containing 1 022 000 mutants, was constructed and kindly provided by Gemma Langridge (The Wellcome Trust Sanger Institute). Transformation of the SL1344 TraDIS library with the *ramA* GFP reporter plasmid (pMW82p*ramA*) was done using electroporation. Bacteria that expressed greater levels of GFP compared to the negative controls (see below) were identified using a BD FACSAria2 (BD Biosciences). Cells were excited using a 488 nm wavelength laser; forward scatter (FSC), side scatter (SSC) and green fluorescence (via a 502 LP mirror and 530/30 BP filter) were measured. Bacteria were gated from noise using a FSC versus SSC plot. Positive and negative controls were pMW82p*ramA* in SL1344 *ramR::aph* (this over-expresses *ramA* and will give a high GFP reading) and SL1344 *ramA::aph* (gives a 'baseline' GFP level and prevents any auto-induction by RamA). Cells expressing high levels of GFP compared to the negative control were sorted and collected. These sorted cells were grown overnight aerobically at 37°C on LB agar containing ampicillin (50 μg/ml). To confirm greater GFP expression random colonies were taken and fluorescence assays done using a FluoSTAR OPTIMA (BMG Labtech) plate reader as described previously (16). DNA sequencing with transposon specific primers determined sites of transposon insertion.

Determination of gene expression

The effect of loss of *csrA* on the expression of genes encoding other XylS-AraC transcriptional activators, *ramA, marA, soxS*, *rob* and of the efflux pump components *acrA* and *acrB* were measured with real-time quantitative RT-PCR as described by Blair *et al*. (17).

Western blotting

Cell pellets were re-suspended in 50 mM Tris/HCl (pH 8.0) and sonicated (4 30 s pulses with a 30 s pause between each pulse) on ice using an MSE Soniprep 150 (Sanyo, UK). A Bradford assay was done to quantify protein concentration and 10 μg of protein was electrophoresed on 4–12% NuPAGE® Bis-Tris mini gels in NuPAGE® MES SDS running buffer (Life Technologies, UK). Proteins were transferred to a PVDF membrane (Amersham) by electrophoresis for 3 h at 4°C and the membrane blocked with 5% non-fat milk solution. After overnight incubation with antibodies for AcrA, AcrB or FLAG, membranes were washed overnight and incubated with an HRP-linked anti-rabbit secondary antibody (GE Healthcare). The Enhanced chemiluminescence (ECL) western blotting detection system (GE Healthcare) was used to identify bound antibody.

Purification of CsrA-HisX6 protein

Plasmid pCSB12 containing *csrA* cloned into the NdeI and BamHI sites of pET21a+ (Inovagen) was kindly donated to us by Tony Romeo (University of Florida, USA). In order to prevent contamination by the RNA binding protein Hfq in the purification procedure, pCSB12 was transformed into BL21 (DE3) pLysE (Invitrogen) cells in which the *hfq* gene had been deleted. The BL21 (DE3) pLysE/*hfq::aph* strain containing pCSB12 was cultured at 37°C in LB broth with vigorous shaking until an $OD_{600\,nm}$ of 0.6 was attained. Expression of CsrA-HisX6 was induced for 5 h by adding Isopropyl β-D-1- thiogalactopyranosid (IPTG) to a final concentration of 1 mM. Cells were harvested by centrifugation (4000 × *g* for 20 min at 4°C) and the cell pellet was frozen at −20°C until further use. Purification of CsrA-HisX6 was done using a QIAexpress® Ni-NTA spin kit (Qiagen). Briefly, the cell pellet was thawed on ice for 15 min and re-suspended in 10 ml native lysis buffer. After incubation on ice for a further 30 min cell debris was removed by centrifugation (14000 × *g* for 30 min at 4°C). The cell lysate was then applied to a Fast Start Column contain-

ing re-suspended resin. The flow through fraction was collected and stored at −20°C. The column was washed twice with 4 ml of native Wash Buffer with each wash fraction being collected and stored at −20°C. Bound CsrA-HisX6 tagged protein was eluted with two 1 ml aliquots of Native Elution Buffer. Each elution fraction was collected separately and stored at −20°C. All fractions were analyzed by sodium dodecyl sulphate-polyacrylamide gel electrophoresis and Coomassie Blue staining as well as western blotting with anti-His tag antibody (Thermo Fisher Scientific). The second elution fraction was also analyzed by Fourier transform ion cyclotron resonance (FT-ICR) mass spectrometry (Supplementary Table S3) and was used for all the subsequent *in vitro* experiments. The CsrA-HisX6 concentration was estimated using the Bradford protein assay (18).

RNA electrophoretic mobility shift assays

Known binding sites for CsrA were sought based upon data described by Kulkarni *et al.,* (10). RNA transcripts corresponding to the promoter regions of *acrAB* (including wild-type and those harboring site directed mutations), and *ramA* were synthesized *in vitro* using the AmpliScribe™ T7-*Flash*™ Transcription Kit (Cambio Ltd, UK) and purified by ammonium acetate precipitation. Concentrations of transcripts were determined with the Qubit™ fluorometric quantitation system (Life Technologies, UK). The electrophoretic mobility shift assay was done using an electrophoretic mobility shift assay (EMSA) kit (E33075; Thermo Fisher, UK) according to the manufacturer's instructions. Briefly, 0.5 nM target RNA was incubated with CsrA-HisX6 protein for 20 min at room temperature in a 15 μl reaction mixture containing 1 × binding buffer (750 mM KCl, 0.5 mM dithiothreitol, 0.5 mM ethylenediaminetetraacetic acid (EDTA), 50 mM Tris–HCl, pH 7.4). Following addition of EMSA gel-loading solution, mixtures were separated by electrophoresis on a non-denaturing 8% (wt/vol) polyacrylamide gel in 0.5 × TBE buffer (22 mM Tris-HCl, 22 mM boric acid, 0.5 mM EDTA, pH 8.0). Gels were stained with 1 × SYBR Green EMSA nucleic acid stain. DNA was then visualized using a G:BOX F3 gel documentation system (Syngene, UK).

Construction of the AcrA::GFP translational reporter fusion

A 1525-bp DNA fragment containing *acrA* and its promoter region was amplified from SL1344 genomic DNA using PCR primers 5′-GGGGGATCCGCTCCCAGATCT CACTGAAT-3′ and 5′-GGGGTACCAGACCTGGGCT GAGCAGGTTG-3′. This PCR product was cloned in BamHI/KpnI digested pDOC-G (19), to form the translational fusion plasmid pAcrA-TF.

Site-directed mutagenesis of the CsrA binding sites in the *acrAB* leader region

For our initial CsrA binding experiments the GGA motifs in the CsrA binding sites in the leader sequence of *acrAB* were mutated to GTA using the QuikChange Site Directed Mutagenesis kit (Stratagene). The G to T substitutions were introduced into the *acrAB* leader sequence on pMW82p*acrAB and* pCR®II-p*acrAB* resulting in plasmids, pMW82p*acrAB* (CsrA BS-SDM) and pCR®II- p*acrAB* (CsrA BS-SDM). To investigate the role of RNase E degradation, nucleotides in the *acrAB* leader sequence, which contain putative RNase E cleavage sites, were deleted using the QuikChange Site Directed Mutagenesis kit (Stratagene). The resulting plasmid was pMW82p*acrAB* (RNase E- DEL). To assess positive regulation of AcrAB expression by CsrA nucleotide substitutions were made in the CsrA binding regions. Two sets of nucleotide substitutions were made; 5′-TAAGGAC-3′ to 5′-GCTATGT-3′ and 5′-TCGGAC-3′ to 5′-GTCTGA-3′. Nucleotide substitutions were made using the QuikChange Lightning Multi Site-Directed Mutagenesis Kit (Stratagene).

In vitro coupled transcription-translation assay

Plasmid pT7-*acrA*-GFP contains a T7 promoter driving transcription of an *acrA*-GFP translational fusion. Plasmid pT7-*acrA*-GFP Mut CsrA BS is identical to pT7-*acrA*-GFP except that it contains TAAGGAC to GCTATGT and TCGGAC to GTCTGA mutations in the two predicted CsrA binding sites in the leader sequence of *acrA*. Both plasmids were purified using the Plasmid Midiprep Kit (Qiagen) followed by phenol/chloroform extraction and ethanol precipitation. These two plasmids were used as the templates for coupled transcription-translation reactions using the PURExpress® *In Vitro* Protein Synthesis Kit (New England BioLabs). Reaction mixtures containing 50 ng plasmid DNA template in the absence and presence of 320 nM of purified His-tagged CsrA were incubated for 2 h at 37°C. Fluorescence was measured at excitation and emission wavelengths of 492 and 520 nm, respectively, using a FLUOstar Optima (BMG labtech).

RNA secondary structure prediction of wild-type and mutated *acrAB* transcripts

The RNA secondary structures of wild-type and mutated *acrAB* RNA transcripts were predicted with ViennaRNA Package 2.0 (20).

mRNA stability assay

Strains were cultured at 37°C in LB medium to $OD_{600\,nm}$ of 0.8 and treated with rifampicin (200 μg/ml) to inhibit transcription (21). After 0, 1, 2, 3, 4 and 5 min of rifampicin treatment cells were harvested by centrifugation (4000 × *g*) and RNA extracted using the Wizard SV RNA kit (Promega, UK). The amount of *acrB, ramA* and *gfp* mRNA in each sample was determined by real-time quantitative RT-PCR as described by Blair *et al.*, (17). The percentage of RNA remaining at each time-course was determined by calculating the difference in cycle threshold (ΔCT) compared to the 0-min time point after taking into account 16S rRNA levels, as per manufacturer's instructions (Bio-Rad, UK).

Induction assays

To observe induction of AcrAB from our translational GFP reporter construct in SL1344 and SL1344 *csrA::aph* we

measured fluorescence following the addition of 2 mM indole, using the method described by Lawler *et al*., (4). Two biological and three technical replicates of each culture were used in each assay. Simultaneous measurement of fluorescence at excitation and emission wavelengths of 492 and 520 nm, respectively, and absorbance at a wavelength of 600nm was carried out in a FLUOstar Optima (BMG labtech) at an incubation temperature of 37°C.

Growth kinetics and determination of susceptibility to antimicrobials

Growth rates in LB broth or minimal medium (Teknova, USA) were determined over 24 h at 37°C using a FLUOstar OPTIMA (BMG Labtech, UK) plate reader as previously described (22). The minimum inhibitory concentration of each antimicrobial tested was determined by the standardized agar doubling-dilution method as described previously by the BSAC (http://www.bsac.org.uk) (23).

Biofilm formation and curli synthesis

Biofilm formation and curli synthesis by SL1344, SL1344 *csrA::aph* and SL1344 *csrA::aph* pWSK30*csrA* was determined as described previously by Baugh *et al*., (24).

Adhesion and invasion assays

The ability of strains to adhere to, and invade, INT 407 (human embryonic intestine cells) was measured as previously described (25). Each assay was repeated a minimum of three times, with each experiment including four technical replicates per bacterial strain.

Statistical analysis

Data obtained in this study are from at least three independent experiments and are shown as means ± standard deviation. Statistical significance was determined with the Students *t*-test where $P < 0.05$ was regarded as statistically significant.

RESULTS

A screening assay with a GFP reporter identified CsrA as a potential regulator of *ramA*

A *S.* Typhimurium SL1344 transposon library was used to identify factors important for *ramA* expression. Briefly, the library was transformed with plasmid pMW82p*ramA* encoding an unstable GFP derivative under the control of the *ramA* promoter. Cells with increased GFP fluorescence, compared to a negative control, were isolated using FACS (Figure 2) and cultured on LB agar. Twenty colonies were selected and for the eight isolates showing the greatest fluorescence we identified *csrA* ($n = 2$), *flgL* ($n = 1$), *ccmA* ($n = 2$), *ccmB* ($n = 1$) and *alaS* ($n = 2$) as the site of transposon insertion. Since CsrA has a known role in controlling gene expression we focused on this factor.

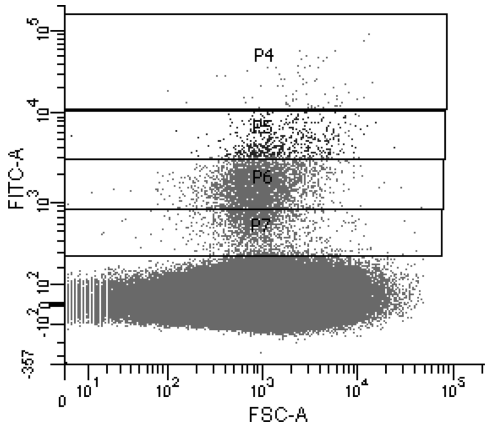

Figure 2. Output from FACS following transformation of pMW82-p*ramA* into *Salmonella enterica serovar* Typhimurium transposon library post 2 h recovery incubation at 37°C. Cell populations expressing greater GFP than the negative control were gated into populations P4, P5, P6 and P7 before sorting.

csrA inactivation affects growth, biofilm formation and virulence but does not affect susceptibility to antimicrobials

A SL1344 *csrA::aph* mutant was constructed and to check that it behaved as expected we investigated the properties of this mutant. Consistent with previous observations (26–28) the SL1344 *csrA::aph* mutant was defective for both planktonic growth and biofilm formation. Furthermore, these phenotypes were reversed upon complementation with wild-type *csrA* (Supplementary Table S2). Inactivation of *csrA* also attenuated the virulence of *Salmonella* (Supplementary Figure S2) but no difference in susceptibility to tested antimicrobials was observed (Supplementary Table S2).

Absence of *csrA*/CsrA increases expression of transcriptional activators but not efflux pump components

Transcription of *ramA* in SL1344 *csrA::aph* increased by 4.2 ± 1.6-fold (Table 1). Since RamA activates *acrAB* expression, we reasoned that expression of these genes should also increase in cells lacking *csrA*. Hence, the plasmid pMW82p*acrAB* was used to transform SL1344 *csrA::aph* or the parent strain. Surprisingly, loss of *csrA* caused no increase in *acrAB* transcription (1.16 ± 0.88-fold) (Table 1). These observations were confirmed by real-time quantitative RT-PCR (Table 1) whilst western blotting indicated reduced translation of AcrA and AcrB (Figure 3A and B). Interestingly, expression of *marA* and *soxS* increased in cells lacking *csrA* (Table 1).

CsrA binds to the leader region of *acrAB* but not to *ramA*

The lack of *acrAB* induction led us to question why *ramA* expression increased in the SL1344 *csrA::aph* mutant. In previous work, we showed that increased expression of *ramA* occurs when *acrAB* is inactivated (4,29). Therefore, we hypothesized that CsrA may influence *ramA* expression indirectly by targeting expression of *acrAB*. This model would explain the negative correlation between *ramA* and

Table 1. Gene and protein expression of efflux pump components and regulators in SL1344 *csrA::aph* and MDR *S*. Typhimurium and their respective *csrA* mutants

Gene/protein	SL1344 *csrA::aph*			SL1344 *ramR::aph*	SL1344 Δ*ramR*/*csrA::aph*	SL1344 MDR mutant	SL1344 MDR mutant/*csrA::aph*
	Fold change in gene/protein expression compared to SL1344						
	GFP	RT-PCR	Protein	RT-PCR	RT-PCR	RT-PCR	RT-PCR
***ramA*/RamA**	**4.2 ± 1.6***	**3.8 ± 1.8***	**24.5***	**3.8 ± 0.2***	**4.9 ± 0.2***	**3.1 ± 0.1***	**4.1 ± 0.3***
acrAB	1.2 ± 0.9	ND	ND	ND	ND	ND	ND
***acrA*/AcrA**	ND	1.02 ± 0.04	*0.2**	**2.7 ± 0.2***	**2.8 ± 0.1***	**2.5 ± 0.2***	**2.2 ± 0.2***
***acrB*/AcrB**	ND	1.03 ± 0.03	*0.2**	**3.9 ± 0.2***	**3.7 ± 0.3***	**3.2 ± 0.2***	**3.1 ± 0.3***
marA	ND	**3.1 ± 1.4***	ND	ND	ND	ND	ND
soxS	ND	**4.1 ± 1.1***	ND	ND	ND	ND	ND
csrA	ND	ND	ND	1.1 ± 0.03		1.03 ± 0.03	

GFP expression data were obtained from fluorescence assays performed with the *ramA* and *acrAB* GFP transcriptional fusions as described in the 'Materials and Methods' section. RT-PCR expression data was obtained by using a real-time quantitative method as described by Blair *et al*., (17). Protein expression data was obtained by western blotting and fold change expression data relates to data described in Figure 3. Values were calculated from three biological replicates; ±standard deviation, $*P < 0.05$ by Student's *t*-test, Increased expression, bold font; decreased expression, italics. ND, not done.

acrAB expression in cells lacking CsrA. Furthermore, reduced efflux would be consistent with enhanced expression of *marA* and *soxS* described above (Table 1). Consistent with our model, only a putative secondary CsrA binding site could be identified in the *ramA* mRNA leader (Figure 4A) and this was insufficient to bind CsrA *in vitro* (Figure 5A). Conversely, analysis of the *acrAB* promoter sequence identified both primary (AAGGA) and secondary (TCGGA) CsrA targets (Figure 4B) that bound CsrA tightly (Figure 5B). A non-linear least squares analysis of the data revealed a K_d value of 46.27 ± 3.7 nM (Figure 5D). To establish whether the putative CsrA binding sites were responsible for the observed mobility shift the sites AAGGA and TCGGA were mutagenized to AAGTA and TCGTA, respectively. No mobility shift was observed with these control RNA templates (Figure 5C). Furthermore, mutation of the CsrA binding sites in the *acrAB* mRNA leader reduced expression of downstream-encoded GFP 3.2-fold.

CsrA positively regulates AcrAB protein levels by stabilizing *acrAB* mRNA

CsrA primarily regulates gene expression by preventing translation initiation (14). Our data suggest that CsrA is a positive regulator of *acrAB*. As a first step toward understanding this positive regulation we considered the possibility that CsrA might stabilize the *acrAB* mRNA. Hence stability of the *acrAB* transcript was quantified in SL1344 or the *csrA::aph* derivative. Five minutes after the addition of rifampicin, which inhibits transcription initiation, most *acrAB* mRNA remained in SL1344 cells. Conversely, a 2-fold reduction in *acrAB* mRNA was observed in the absence of CsrA (Figure 6A). Mutation of the *acrAB* CsrA binding sites on the translational fusion, pAcrA-TF-SDM, had a similar but smaller effect on the stability of *acrA-gfp* transcript (Figure 6B).

CsrA promotes efficient translation of AcrAB

In order to further determine whether CsrA enhances *acrAB* translation we used the *in vitro* coupled transcription-translation PURExpress system. Two plasmid constructs, one carrying an *acrA*-GFP translational fusion with wildtype leader sequence and another carrying an *acrA*-GFP translational fusion with mutated CsrA binding sites were used in this analysis. Expression from each construct was measured by determining fluorescence. Addition of CsrA-His6X to the system caused a 1.32 ± 0.02-fold increase in expression of the *acrA*-GFP construct, containing the wildtype leader sequence. In contrast, expression of the *acrA*-GFP translational fusion with mutated CsrA binding sites construct was not significantly changed in the presence of CsrA-His6X compared to expression observed in the absence of CsrA-His6X (Figure 7). We conclude that CsrA directly stabilizes the *acrAB* mRNA and that bound CsrA enhances translation of AcrAB. These data also suggest that the effect of CsrA on *acrB* mRNA stability (Figure 6A and B) was a consequence of RNA secondary structure. We reasoned that CsrA might alter *acrAB* mRNA structure to enhance translation and transcript stability. To understand the likelihood of this scenario, we predicted secondary structure of the *acrAB* mRNA leader sequence. The prediction suggests extensive intramolecular base pairing that occludes both the ribosome binding site and the CsrA targets (Figure 8A–C). Binding of CsrA is likely to disrupt this repressive RNA structure. If this model is correct, it should be possible to mutate the *acrAB* mRNA so that intramolecular base pairing is reduced and the requirement for CsrA is relieved. Fortuitously, the mutations described above, that ablate the CsrA binding sites, are also expected to reduce intramolecular base pairing. Hence, we predicted that disrupting the CsrA target sequences in cells lacking CsrA should have a positive effect on *acrA-gfp* expression. As predicted, mutation of the CsrA binding sites caused increased GFP expression in the SL1344 *csrA::aph* mutant (Figure 9). These data also explain why the effect of mutating the CsrA targets has a smaller effect than deleting the CsrA gene; the mutations simultaneously ameliorate CsrA binding and intramolecular base pairing.

Indole induces AcrAB to a greater degree in the presence of CsrA

Previous work has shown that the *acrAB* locus in *Salmonella* is induced by indole (4,30,31). This induction is dependent on RamA and requires the binding of RamA to a binding sequence (*ram*-box) located upstream of *acrA*

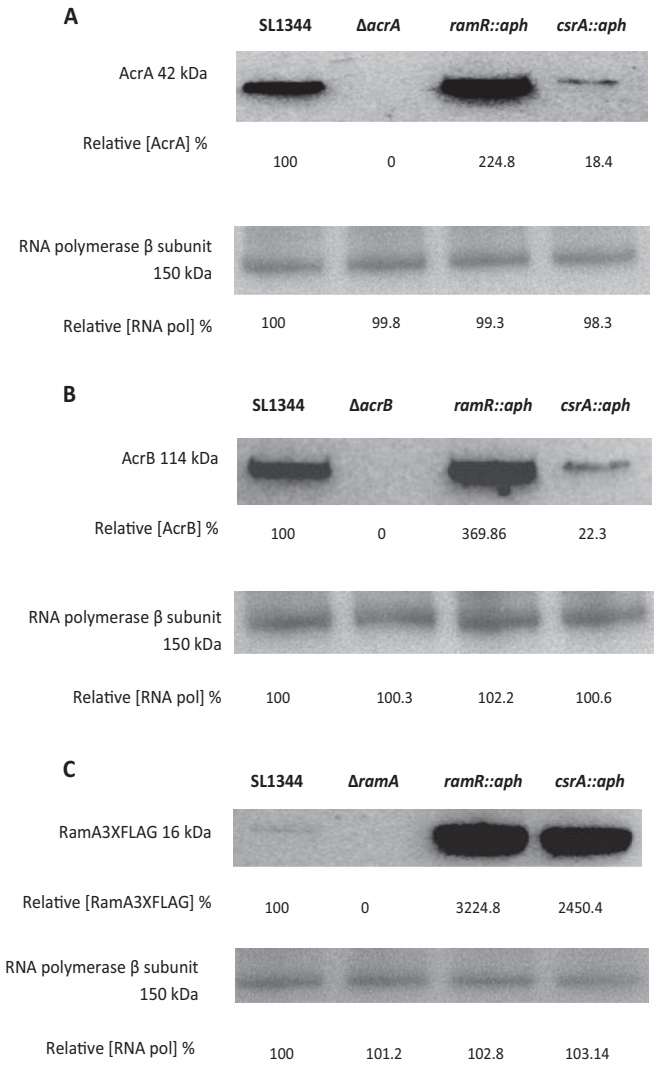

Figure 3. Effect of *csrA* inactivation on protein levels of AcrA, AcrB and RamA3XFLAG. (**A**) Expression of AcrA in SL1344 (WT), Δ*acrA*, *ramR::aph* and *csrA::aph* mutants. (**B**) Expression of AcrB in SL1344 (WT), Δ*acrB, ramR::aph* and *csrA::aph* mutants. (**C**) Expression of RamA3XFLAG in SL1344 (WT), Δ*ramA, ramR::aph* and *csrA::aph* mutants. Internal control used in all the experiments was the β subunit of RNA polymerase. The RNA polymerase western blot confirms that there is an equal amount of protein in each well. Band intensity was determined using GeneSys, this information was used to assign a relative concentration of AcrA, AcrB and RamA3XFLAG to each respective band, expressed as a percentage of wild-type. For negative controls, the respective deleted gene mutant i.e. Δ*acrA*, Δ*acrB* and Δ*ramA* mutants, were used.

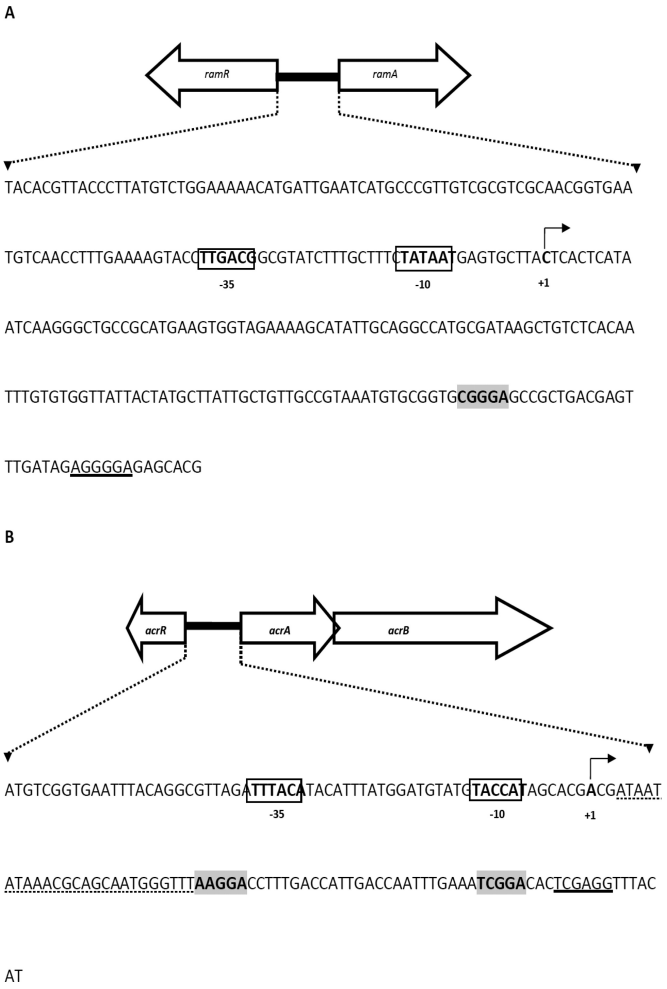

Figure 4. DNA sequence of the *ramA* and *acrAB* promoter regions used in this study. (**A**) DNA sequence of the *Salmonella enterica serovar* Typhimurium (SL1344) 288 bp *ramRA* intergenic region. The *ramA* promoter −10 and −35 elements, and transcription start site (TSS) are in bold type. The ribosomal binding site is underlined and the putative CsrA binding site is in bold and shaded gray. (**B**) DNA sequence of the *S*. Typhimurium (SL1344) 141 bp *acrAB* promoter region. The *acrAB* promoter −10 and −35 elements, and predicted TSS are in bold type. The ribosomal binding site is underlined and the putative CsrA binding sites are in bold and shaded gray. The deleted sequence containing putative RNase E cleavage sites is indicated with dotted lines.

(31). To investigate the role CsrA we compared induction of *acrAB* by indole in SL1344 and the *csrA::aph* derivative; induction was reduced in the absence of CsrA (Figure 10).

Deletion of *csrA* in a MDR mutant confers a more susceptible phenotype

As noted above deletion of *csrA* has little effect on antibiotic sensitivity in wild-type *Salmonella*. However, since over-expression of AcrAB is important for multidrug resistance, we set out to determine if loss of *csrA* from multidrug resistant *S*. Typhimurium strains might have a more prominent effect. Susceptibility to ciprofloxacin, nalidixic acid, tetracycline and chloramphenicol in two MDR mutants (SL1344Δ*ramR* and SL1344MDR) lacking *csrA* was increased by between 2- and 4-fold (Supplementary Table S2). We also determined the impact of *csrA* deletion on drug efflux. Our data showed that ethidium bromide efflux in the MDR mutants lacking *csrA* was slower than in the respective parent strains (Supplementary Figure S3). Consistent with our model for regulation of *acrAB* translation by CsrA we observed no difference in *acrAB* transcript levels in MDR *Salmonella* mutants lacking *csrA* whilst *ramA* transcription was enhanced (Table 1). However, levels of AcrB in the *S*. Typhimurium MDR mutants were reduced in the absence of CsrA (Figure 11).

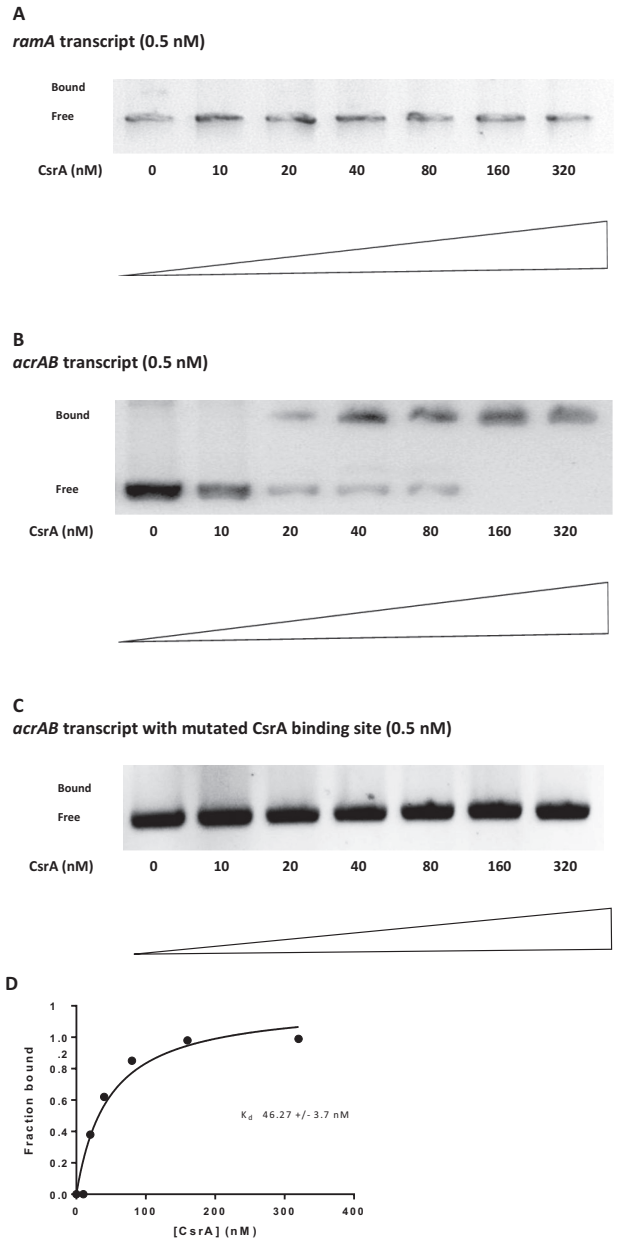

Figure 5. RNA electrophoretic mobility shift analysis to evaluate *ramA* and *acrAB* RNA interactions with CsrA. (**A**) *In vitro* transcribed *ramA* RNA (0.5 nM) was incubated with the various concentrations of CsrA indicated at the bottom of each lane. The positions of bound and free RNA are shown at the left of each panel. (**B**) *In vitro* transcribed *acrAB* RNA (0.5 nM) was incubated with the various concentrations of CsrA indicated at the bottom of each lane. The positions of bound and free RNA are shown at the left of each panel. (**C**) Effect of mutating putative CsrA binding sites on CsrA-*acrAB* RNA interactions. RNA electrophoretic mobility shift assays were performed using mutant *acrAB* RNA (0.5 nM). The concentration of CsrA was indicated at the bottom of each lane. The positions of bound and free RNA are shown. (**D**) Binding curve for the reaction shown in B.

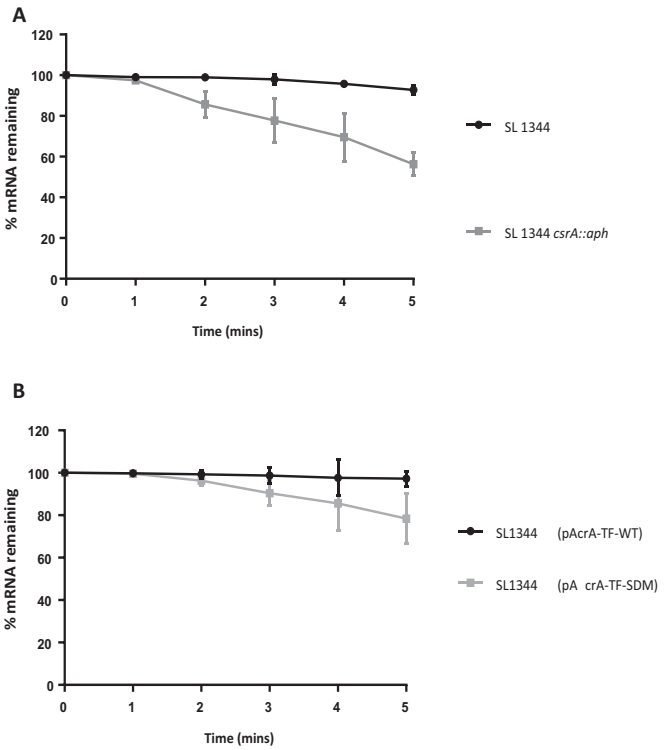

Figure 6. Absence of CsrA and CsrA binding sites on *acrB* and acrA-*gfp* mRNA stability. (**A**) Analysis of acrB mRNA stability in *Salmonella enterica serovar* Typhimurium wild-type and *csrA* mutant strain. (**B**) Analysis of *acrA-gfp* mRNA stability in *S.* Typhimurium containing pAcrA-TF-WT and pAcrA-TF-SDM translational GFP fusions.

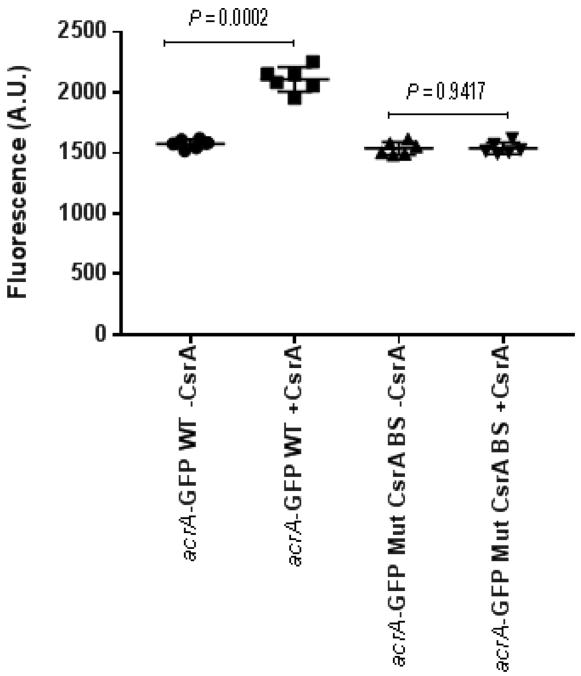

Figure 7. Effect of CsrA on *acrA*-GFP translation. Coupled transcription-translation reactions were performed with a PURExpress kit using pT7-*acrA*-GFP and pT7-*acrA*-GFP Mut CsrA BS translational fusions in the presence and absence of purified CsrA-His protein (320 nM). Fluorescence was measured at excitation and emission wavelengths of 492 and 520 nm, respectively using a FLUOstar Optima. Each experiment was performed three times.

DISCUSSION

In this study, we show that CsrA binds to and stabilizes the *acrAB* mRNA. From our *in silico* data, we propose a mechanism whereby CsrA binding prevents formation of a re-

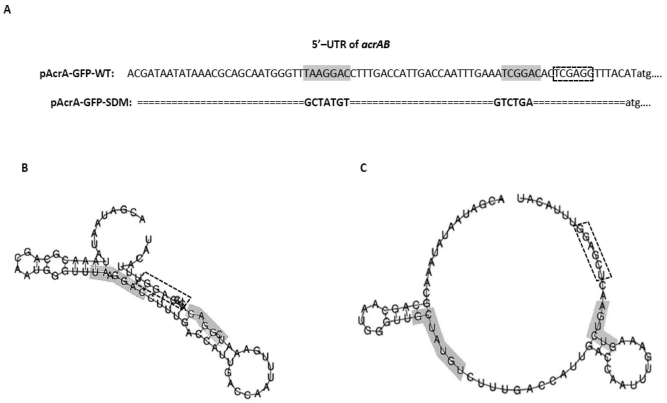

Figure 8. Primary sequence and secondary RNA structures of WT and mutant *acrAB* leader regions. Primary DNA sequence of wildtype 5′ UTR of *acrAB* and mutated 5′ UTR of *acrAB* in which the nucleotides making up the CsrA binding sites have been substituted (gray shaded box). Ribosome binding site (dashed rectangle box). (**A**) The RNA structures of the *acrAB* upstream region in the two plasmids of pAcrA-GFP-WT (**B**) and pAcrA-GFP-SDM (**C**) were predicted by RNAfold and their folding free energies were −12.30 kcal/mol and −6.0 kcal/mol, respectively. (Substituted nucleotides in gray shaded box)

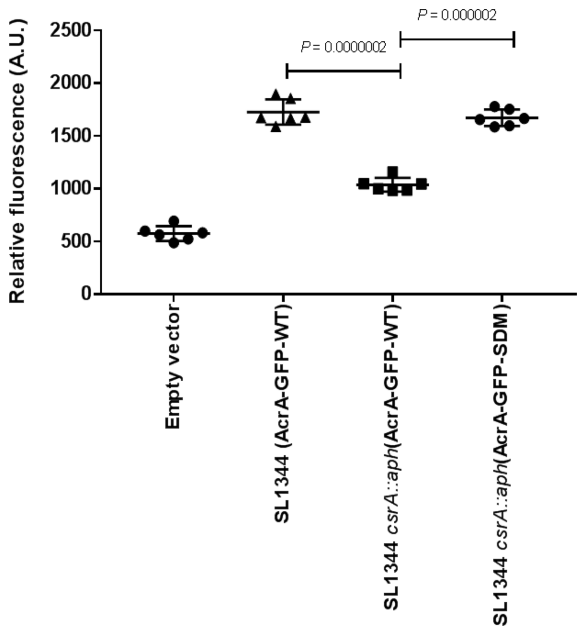

Figure 9. AcrA-GFP expression from the wildtype and mutated *acrAB* leader region. GFP expression from the wildtype (pAcrA-GFP-WT) and mutated (pAcrA-GFP-SDM) translational fusions in SL1344 and SL1344 *csrA::aph*. GFP levels were calculated from three biological replicates; error bars indicate the standard deviation.

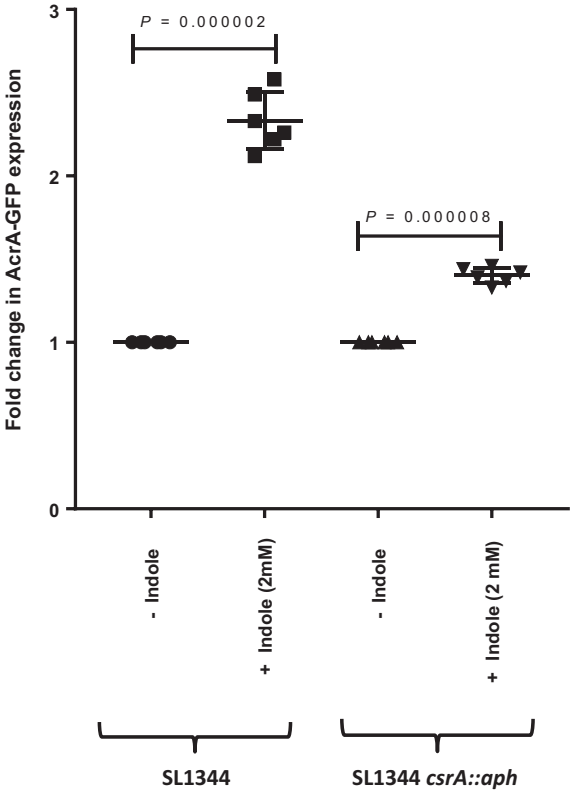

Figure 10. Induction of AcrB in SL1344 and SL1344 *csrA::aph* in the presence of 2 mM indole. GFP levels were calculated from three biological replicates; error bars indicate the standard deviation.

pressive RNA structure that impedes binding of the ribosome. To date there are only a few examples of CsrA, or its homologue RsmA, acting to increase gene expression. For example, in *E. coli* CsrA positively regulates *flhDC* by binding two sites in the *flhDC* mRNA leader that prevent transcript cleavage by RNase E (21). At the *E. coli moaA* locus, the *moa* mRNA leader sequence contains two CsrA-binding sites and also constitutes a molybdenum cofactor-sensing riboswitch. This mechanism is the first example of a riboswitch aptamer that interacts with two regulatory factors, a ligand and an RNA binding protein. Two studies have suggested a mechanism of activation whereby CsrA blocks the formation of an inhibitory structure at the RNA 5′ end (32,33). Although implied, these studies did not directly show the effect CsrA or RsmA had on mRNA stability. Here, we have shown that CsrA plays an important role in stabilizing *acrB* mRNA and thus promoting optimal translation of AcrAB. Our data show that binding of CsrA to the *acrAB* transcript alters RNA structure and we propose that this makes the ribosome binding site more accessible in a similar manner to that described previously by Ren *et al*. for the action of RsmA at the *Pseudomonas aeruginosa* phenazine biosynthetic gene clusters, *phz1* and *phz2*, (33). Our data from indole induction experiments suggests that CsrA is required for optimal AcrAB expression in response to a stimulus.

This is the first example of CsrA regulating the expression of an RND type efflux pump in any bacterium. Understanding the molecular basis of intrinsic and acquired MDR via efflux pumps is essential if new drugs are to be discovered that are not susceptible to this mechanism (http://www.pewtrusts.org/~/media/assets/2016/05/ascientificroadmapforantibioticdiscovery.pdf). Identifying factors that could be inhibited and so reduce efflux could form the basis of a drug discovery program. We postulate that CsrA is a potential new drug target.

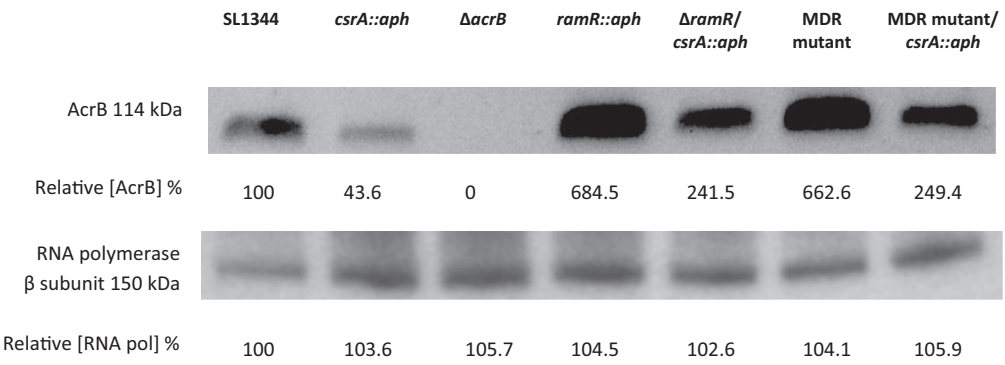

Figure 11. AcrB expression levels in SL1344, MDR mutants of SL1344 and respective *csrA* mutants. Expression of AcrB in SL1344 (WT), *csrA::aph, ΔacrB, ramR::aph, ΔramR/ csrA::aph*, MDR mutant and MDR mutant/*csrA::aph*. Internal control used in the experiment was the β subunit of RNA polymerase. The RNA polymerase Western blot confirms that there is an equal amount of protein in each well. Band intensity was determined using GeneSys, this information was used to assign a relative concentration of AcrB to each band, expressed in percentage of wild-type. A Δ*acrB* mutant was used as a negative control.

SUPPLEMENTARY DATA

Supplementary Data are available at NAR Online.

ACKNOWLEDGEMENTS

We thank Prof. Tony Romeo for providing us with strain PLB328 for CsrA-HisX6 protein production. We would also like to thank Gemma Langridge for providing the *S. typhimurium* SL1344 TraDIS library.

FUNDING

Medical Research Council (MRC) Programme Grant [GO501415 to L.J.V.P.]. Funding for open access charge: MRC [GO501415].
Conflict of interest statement. None declared.

REFERENCES

1. Piddock,L.J. (2006) Clinically relevant chromosomally encoded multidrug resistance efflux pumps in bacteria. *Clin. Microbiol. Rev.*, **19**, 382–402.
2. Ricci,V., Tzakas,P., Buckley,A. and Piddock,L.J. (2006) Ciprofloxacin-resistant *Salmonella enterica* serovar Typhimurium strains are difficult to select in the absence of AcrB and TolC. *Antimicrob. Agents Chemother.*, **50**, 38–42.
3. Martin,R.G. and Rosner,J.L. (2002) Genomics of the *marA*/*soxS*/*rob* regulon of *Escherichia coli*: identification of directly activated promoters by application of molecular genetics and informatics to microarray data. *Mol. Microbiol.*, **44**, 1611–1624.
4. Lawler,A.J., Ricci,V., Busby,S.J. and Piddock,L.J. (2013) Genetic inactivation of *acrAB* or inhibition of efflux induces expression of *ramA*. *J. Antimicrob. Chemother.*, **68**, 1551–1557.
5. Agaras,B., Sobrero,P. and Valverde,C. (2013) A CsrA/RsmA translational regulator gene encoded in the replication region of a *Sinorhizobium meliloti* cryptic plasmid complements *Pseudomonas fluorescens rsmA*/*E* mutants. *Microbiology*, **159**, 230–242.
6. Babitzke,P., Baker,C.S. and Romeo,T. (2009) Regulation of translation initiation by RNA binding proteins. *Annu. Rev. Microbiol.*, **63**, 27–44.
7. Dubey,A.K., Baker,C.S., Romeo,T. and Babitzke,P. (2005) RNA sequence and secondary structure participate in high-affinity CsrA-RNA interaction. *RNA*, **11**, 1579–1587.
8. Mercante,J., Suzuki,K., Cheng,X., Babitzke,P. and Romeo,T. (2006) Comprehensive alanine-scanning mutagenesis of Escherichia coli CsrA defines two subdomains of critical functional importance. *J. Biol. Chem.*, **281**, 31832–31842.
9. Valverde,C., Lindell,M., Wagner,E.G. and Haas,D. (2004) A repeated GGA motif is critical for the activity and stability of the riboregulator RsmY of Pseudomonas fluorescens. *J. Biol. Chem.*, **279**, 25066–25074.
10. Kulkarni,P.R., Jia,T., Kuehne,S.A., Kerkering,T.M., Morris,E.R., Searle,M.S., Heeb,S., Rao,J. and Kulkarni,R.V. (2014) A sequence-based approach for prediction of CsrA/RsmA targets in bacteria with experimental validation in *Pseudomonas aeruginosa*. *Nucleic Acids Res.*, **42**, 6811–6825.
11. Barnard,F.M., Loughlin,M.F., Fainberg,H.P., Messenger,M.P., Ussery,D.W., Williams,P. and Jenks,P.J. (2004) Global regulation of virulence and the stress response by CsrA in the highly adapted human gastric pathogen *Helicobacter pylori*. *Mol. Microbiol.*, **51**, 15–32.
12. Romeo,T., Gong,M., Liu,M.Y. and Brun-Zinkernagel,A.M. (1993) Identification and molecular characterization of *csrA*, a pleiotropic gene from *Escherichia coli* that affects glycogen biosynthesis, gluconeogenesis, cell size, and surface properties. *J. Bacteriol.*, **175**, 4744–4755.
13. Romeo,T., Vakulskas,C.A. and Babitzke,P. (2013) Post-transcriptional regulation on a global scale: form and function of Csr/Rsm systems. *Environ. Microbiol.*, **15**, 313–324.
14. Seyll,E. and Van Melderen,L. (2013) The ribonucleoprotein Csr network. *Int. J. Mol. Sci.*, **14**, 22117–22131.
15. Datsenko,K.A. and Wanner,B.L. (2000) One-step inactivation of chromosomal genes in *Escherichia coli* K-12 using PCR products. *Proc. Natl. Acad. Sci. U.S.A.*, **97**, 6640–6645.
16. Ricci,V., Busby,S.J. and Piddock,L.J. (2012) Regulation of RamA by RamR in *Salmonella enterica* serovar Typhimurium: isolation of a RamR superrepressor. *Antimicrob. Agents Chemother.*, **56**, 6037–6040.
17. Blair,J.M., Smith,H.E., Ricci,V., Lawler,A.J., Thompson,L.J. and Piddock,L.J. (2015) Expression of homologous RND efflux pump genes is dependent upon AcrB expression: implications for efflux and virulence inhibitor design. *J. Antimicrob. Chemother.*, **70**, 424–431.
18. Bradford,M.M. (1976) A rapid and sensitive method for the quantitation of microgram quantities of protein utilizing the principle of protein-dye binding. *Anal. Biochem.*, **72**, 248–254.
19. Lee,D.J., Bingle,L.E., Heurlier,K., Pallen,M.J., Penn,C.W., Busby,S.J. and Hobman,J.L. (2009) Gene doctoring: a method for recombineering in laboratory and pathogenic Escherichia coli strains. *BMC Microbiol.*, **9**, 252–265.
20. Lorenz,R., Bernhart,S.H., Honer Zu Siederdissen,C., Tafer,H., Flamm,C., Stadler,P.F. and Hofacker,I.L. (2011) ViennaRNA Package 2.0. *Algorithms Mol. Biol.*, **6**, 26–39.
21. Yakhnin,A.V., Baker,C.S., Vakulskas,C.A., Yakhnin,H., Berezin,I., Romeo,T. and Babitzke,P. (2013) CsrA activates *flhDC* expression by protecting *flhDC* mRNA from RNase E-mediated cleavage. *Mol. Microbiol.*, **87**, 851–866.
22. Ricci,V. and Piddock,L.J. (2009) Ciprofloxacin selects for multidrug resistance in *Salmonella enterica* serovar Typhimurium mediated by at least two different pathways. *J. Antimicrob. Chemother.*, **63**, 909–916.

23. Andrews,J.M., Howe,R.A. and Testing,B.W.P.o.S. (2011) BSAC standardized disc susceptibility testing method (version 10). *J. Antimicrob. Chemother.*, **66**, 2726–2757.
24. Baugh,S., Phillips,C.R., Ekanayaka,A.S., Piddock,L.J. and Webber,M.A. (2014) Inhibition of multidrug efflux as a strategy to prevent biofilm formation. *J. Antimicrob. Chemother.*, **69**, 673–681.
25. Buckley,A.M., Webber,M.A., Cooles,S., Randall,L.P., La Ragione,R.M., Woodward,M.J. and Piddock,L.J. (2006) The AcrAB-TolC efflux system of *Salmonella enterica* serovar Typhimurium plays a role in pathogenesis. *Cell Microbiol.*, **8**, 847–856.
26. Altier,C., Suyemoto,M. and Lawhon,S.D. (2000) Regulation of *Salmonella enterica* serovar typhimurium invasion genes by *csrA*. *Infect. Immun.*, **68**, 6790–6797.
27. Lawhon,S.D., Frye,J.G., Suyemoto,M., Porwollik,S., McClelland,M. and Altier,C. (2003) Global regulation by CsrA in *Salmonella typhimurium*. *Mol. Microbiol.*, **48**, 1633–1645.
28. Simm,R., Ahmad,I., Rhen,M., Le Guyon,S. and Romling,U. (2014) Regulation of biofilm formation in *Salmonella enterica* serovar Typhimurium. *Future Microbiol.*, **9**, 1261–1282.
29. Bailey,A.M., Paulsen,I.T. and Piddock,L.J. (2008) RamA confers multidrug resistance in *Salmonella enterica* via increased expression of *acrB*, which is inhibited by chlorpromazine. *Antimicrob. Agents Chemother.*, **52**, 3604–3611.
30. Nikaido,E., Yamaguchi,A. and Nishino,K. (2008) AcrAB multidrug efflux pump regulation in *Salmonella enterica* serovar Typhimurium by RamA in response to environmental signals. *J. Biol. Chem.*, **283**, 24245–24253.
31. Nikaido,E., Shirosaka,I., Yamaguchi,A. and Nishino,K. (2011) Regulation of the AcrAB multidrug efflux pump in Salmonella enterica serovar Typhimurium in response to indole and paraquat. *Microbiology*, **157**, 648–655.
32. Bhatt,S., Edwards,A.N., Nguyen,H.T., Merlin,D., Romeo,T. and Kalman,D. (2009) The RNA binding protein CsrA is a pleiotropic regulator of the locus of enterocyte effacement pathogenicity island of enteropathogenic *Escherichia coli*. *Infect. Immun.*, **77**, 3552–3568.
33. Ren,B., Shen,H., Lu,Z.J., Liu,H. and Xu,Y. (2014) The *phzA*2-G2 transcript exhibits direct RsmA-mediated activation in *Pseudomonas aeruginosa* M18. *PLoS One*, **9**, e89653.